



PATENT
5659-02300
TH1948

CERTIFICATE OF EXPRESS MAIL
UNDER 37 C.F.R. §1.10

"Express Mail" mailing label number: EL822014017US
DATE OF DEPOSIT: April 24, 2001

I hereby certify that this paper or fee is being deposited with the United States Postal Service "Express Mail Post Office to Addressee" service under 37 C.F.R. §1.10 on the date indicated above and is addressed to:

Commissioner for Patents
Box Patent Application
Washington, DC 20231

Brit Baker

**IN SITU THERMAL PROCESSING OF A HYDROCARBON CONTAINING
FORMATION IN A REDUCING ENVIRONMENT**

By:

Scott L. Wellington

Harold J. Vinegar

~~Scott L. Wellington~~

Eric de Rouffignac

~~John M. Karanikas~~

Ilya E. Berchenko

George L. Stegemeier

~~Kevin A. Maher~~

Etuan Zhang

Gordon T. Shahin

~~James L. Menotti~~

~~John M. Coles~~

Thomas D. Fowler

~~Charlie R. Keedy~~

~~Ajay M. Madgavkar~~

~~Martijn van Hardeveld~~

Robert C. Ryan

Lanny Schoeling

~~Fred G. Carl~~



PATENT
5659-02300
TH1948

CERTIFICATE OF EXPRESS MAIL
UNDER 37 C.F.R. §1.10

"Express Mail" mailing label number: EL822014017US
DATE OF DEPOSIT: April 24, 2001

I hereby certify that this paper or fee is being deposited with the United States Postal Service "Express Mail Post Office to Addressee" service under 37 C.F.R. §1.10 on the date indicated above and is addressed to:

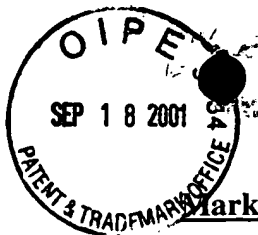
Commissioner for Patents
Box Patent Application
Washington, DC 20231

Brit Baker

**IN SITU THERMAL PROCESSING OF A HYDROCARBON CONTAINING
FORMATION IN A REDUCING ENVIRONMENT**

By:

Scott L. Wellington
Harold J. Vinegar
Eric de Rouffignac
Ilya E. Berchenko
George L. Stegemeier
Etuan Zhang
Gordon T. Shahin
Thomas D. Fowler
Robert C. Ryan

**Marked Up Version of Amendments to Specification**

On page 4, the paragraph beginning on line 16:

Coal is often mined and used as a fuel within an electricity generating power plant. Most coal that is used as a fuel to generate electricity is mined. A significant number of coal formations are, however, not suitable for economical mining. For example, mining coal from steeply dipping coal seams, from relatively thin coal seams (e.g., less than about 1 meter thick), and/or from deep coal seams may not be economically feasible. Deep coal seams include coal seams that are at, or extend to, depths of greater than about 3000 feet (about 914 m) below surface level. The energy conversion efficiency of burning coal to generate electricity is relatively low, as compared to fuels such as natural gas. Also, burning coal to generate electricity often generates significant amounts of carbon dioxide, oxides of sulfur, and oxides of nitrogen that are released into the atmosphere.

On page 5, the paragraph beginning on line 18:

Carbon dioxide may be produced from combustion of fuel and from many chemical processes. Carbon dioxide may be used for various purposes, such as, but not limited to, a feed stream for a dry ice production facility, supercritical fluid in a low temperature supercritical fluid process, a flooding agent for coal bed demethanation, and a flooding agent for enhanced oil recovery. Although some carbon dioxide is productively used, many tons of carbon dioxide are vented to the atmosphere.

On page 17, the paragraph beginning on line 19:

Controlling formation conditions to control the pressure of hydrogen in the produced fluid may result in improved qualities of the produced fluids. In some embodiments it may be desirable to control formation conditions so that the partial pressure of hydrogen in a produced fluid is greater than about 0.5 ~~bar~~bars absolute, as measured at a production well.

On page 18, the paragraph beginning on line 14:

In certain embodiments, a majority of the hydrocarbons in produced fluid may have a carbon number of less than approximately 25. Alternatively, less than about 15 weight % of

the hydrocarbons in the fluid may have a carbon number greater than approximately 25. In other embodiments fluid produced may have a weight ratio of hydrocarbons having carbon numbers from 2 through 4, to methane, of greater than approximately 1 (e.g., for oil shale and heavy hydrocarbons) or greater than approximately 0.3 (e.g., for coal). The non-condensable hydrocarbons may include, but ~~is~~are not limited to, hydrocarbons having carbon numbers less than 5.

On page 29, the paragraph beginning on line 31:

FIGS. 3a-3c depict embodiments of ~~heat sources~~heater wells;

On page 30, the six paragraphs beginning on line 12:

FIG. 11 depicts a portion of an overburden of a formation with a natural distributed combustor heat source;

FIG. 12 and FIG. 13 depict alternate embodiments of a natural distributed combustor ~~heater~~heat source;

FIG. 14 and FIG. 15 depict embodiments of a natural distributed combustor system for heating a formation;

FIGS. 16-~~21~~18 depict several embodiments of an insulated conductor heat source;

FIG. 19 depicts an embodiment of a conductor-in-conduit heat source in a formation;

FIG. 20 depicts an embodiment of a sliding connector;

FIG. 21 depicts an embodiment of a wellhead with a conductor-in conduit heat source;

FIG. 22 and FIGS. 23a-23b depict several embodiments of a centralizer;

FIG. 24 depicts an alternate embodiment of a conductor-in-conduit heat source in a formation;

On page 32, the paragraph beginning on line 10:

FIG. 81 depicts a comparison plot between the average pattern temperature and temperatures at various spots within triangular and hexagonal patterns of heat sources;

On page 32, the twelve paragraphs beginning on line 22:

FIG. 90 depicts pressure versus temperature in an oil shale ~~containing~~ formation during pyrolysis;

FIG. 91 depicts quality of oil produced from an oil shale ~~containing~~ formation;

FIG. 92 depicts ethene to ethane ratio produced from an oil shale ~~containing~~ formation as a function of temperature and pressure;

FIG. 93 depicts yield of fluids produced from an oil shale ~~containing~~ formation as a function of temperature and pressure;

FIG. 94 depicts a plot of oil yield produced from treating an oil shale ~~containing~~ formation;

FIG. 95 depicts yield of oil produced from treating an oil shale ~~containing~~ formation;

FIG. 96 depicts hydrogen to carbon ratio of hydrocarbon condensate produced from an oil shale ~~containing~~ formation as a function of temperature and pressure;

FIG. 97 depicts olefin to paraffin ratio of hydrocarbon condensate produced from an oil shale ~~containing~~ formation as a function of pressure and temperature;

FIG. 98 depicts relationships between properties of a hydrocarbon fluid produced from an oil shale ~~containing~~ formation;

FIG. 99 depicts quantity of oil produced from an oil shale ~~containing~~ formation as a function of partial pressure of H_2 ;

FIG. 100 depicts ethene to ethane ratios of fluid produced from an oil shale ~~containing~~ formation as a function of temperature and pressure;

FIG. 101 depicts hydrogen to carbon atomic ratios of fluid produced from an oil shale ~~containing~~ formation as a function of temperature and pressure;

On page 33, the paragraph beginning on line 15:

FIG. 104 depicts a heat source and production well pattern for a field experiment in an oil shale ~~containing~~ formation;

On page 33, the seven paragraphs beginning on line 18:

FIG. 106 depicts a plot of temperature within the oil shale ~~containing~~ formation during the field experiment;

FIG. 107 depicts pressure within the oil shale ~~containing~~ formation during the field experiment;

FIG. 108 depicts a plot of API gravity of a fluid produced from the oil shale ~~containing~~ formation during the field experiment versus time;

FIG. 109 depicts average carbon numbers of fluid produced from the oil shale ~~containing~~ formation during the field experiment versus time;

FIG. 110 depicts density of fluid produced from the oil shale ~~containing~~ formation during the field experiment versus time;

FIG. 111 depicts a plot of weight percent of hydrocarbons within fluid produced from the oil shale ~~containing~~ formation during the field experiment;

FIG. 112 depicts a plot of an average yield of oil from the oil shale ~~containing~~ formation during the field experiment;

On page 34, the paragraph beginning on line 2:

FIG. 114 depicts total hydrocarbon production and liquid phase fraction versus time of a fluid produced from an oil shale ~~containing~~ formation;

On page 34, the paragraph beginning on line 18:

FIG. 126 depicts yield of oil from a coal ~~containing~~ formation as a function of vitrinite reflectance;

On page 34, the paragraph beginning on line 21:

FIG. 128 depicts CO₂ yield versus atomic O/C ratio for a coal ~~containing~~ formation;

On page 35, the paragraph beginning on line 11:

FIG. 142 depicts weight percent of a hydrocarbon produced from two laboratory experiments on coal from the ~~t~~-field test site versus carbon number distribution;

On page 35, the three paragraphs beginning on line 15:

FIG. 144 depicts percentage ethene to ethane produced from a coal ~~containing~~ formation as a function of heating rate in an experimental field test;

FIG. 145 depicts product quality of fluids produced from a coal ~~containing~~-formation as a function of heating rate in an experimental field test;

FIG. 146 depicts weight percentages of various fluids produced from a coal ~~containing~~-formation for various heating rates in an experimental field test;

On page 35, the five paragraphs beginning on line 23:

FIG. 148 depicts volatiles produced from a coal ~~containing~~-formation in an experimental field test versus cumulative energy content;

FIG. 149 depicts volume of gas produced from a coal ~~containing~~-formation in an experimental field test as a function of time;

FIG. 150 depicts volume of oil produced from a coal ~~containing~~-formation in an experimental field test as a function of energy input;

FIG. 151 depicts synthesis gas production from the coal ~~containing~~-formation in an experimental field test versus the total water inflow;

FIG. 152 depicts additional synthesis gas production from the coal ~~containing~~ formation in an experimental field test due to injected steam;

On page 36, the paragraph beginning on line 13:

FIG. 161 depicts an example of pyrolysis and synthesis gas production stages in a coal ~~containing~~-formation;

On page 36, please delete the paragraph beginning on line 19:

FIG. 165 depicts a plot of cumulative adsorbed methane and carbon dioxide versus pressure in a coal ~~containing~~-formation;

On page 46, the two paragraphs beginning on line 18:

Formation fluids including pyrolyzation fluids may be produced from the formation. The pyrolyzation fluids may include, but are not limited to, hydrocarbons, hydrogen, carbon dioxide, carbon monoxide, hydrogen sulfide, ammonia, nitrogen, water and mixtures thereof. As the temperature of the formation increases, the amount of condensable hydrocarbons ~~of in~~ the produced formation fluid tends to decrease, and the formation will in many instances tend

to produce mostly methane and hydrogen. If a hydrocarbon containing formation is heated throughout an entire pyrolysis range, the formation may produce only small amounts of hydrogen towards an upper limit of the pyrolysis range. After all of the available hydrogen is depleted, a minimal amount of fluid production from the formation will typically occur.

After pyrolysis of hydrocarbons, a large amount of carbon and some hydrogen may still be present in the formation. A significant portion of remaining carbon in the formation can be produced from the formation in the form of synthesis gas. Synthesis gas generation may take place during stage 3 heating as shown in FIG. 1. Stage 3 may include heating a hydrocarbon containing formation to a temperature sufficient to allow synthesis gas generation. For example, synthesis gas may be produced within a temperature range from about 400 °C to about 1200 °C. The temperature of the formation when the synthesis gas generating fluid is introduced to the formation will in many instances determine the composition of synthesis gas produced within the formation. If a synthesis gas generating fluid is introduced into a formation at a temperature sufficient to allow synthesis gas generation, then synthesis gas may be generated within the formation. The generated synthesis gas may be removed from the formation. A large volume of synthesis gas may be produced during generation of synthesis gas-generation.

On page 48, the paragraph beginning on line 1:

A van Krevelen diagram may be useful for selecting a resource for practicing various embodiments described herein (see discussion below). Treating a formation containing kerogen in region 5 will in many instances produce, e.g., carbon dioxide, non-condensable hydrocarbons, hydrogen, and water, along with a relatively small amount of condensable hydrocarbons. Treating a formation containing kerogen in region 7 will in many instances produce, e.g., carbon, condensable and non-condensable hydrocarbons, carbon dioxide, hydrogen, and water. Treating a formation containing kerogen in region 9 will in many instances produce, e.g., methane and hydrogen. A formation containing kerogen in region 7, for example, may in many instances be selected for treatment because doing so will tend to produce larger quantities of valuable hydrocarbons, and lower quantities of undesirable products such as carbon dioxide and water, since the region 7 kerogen has already undergone

dehydration and/or decarboxylation over geological time. In addition, region 7 kerogen can also be further treated to make other useful products (e.g., methane, hydrogen, and/or synthesis gas) as such kerogen transforms to region 9 kerogen.

On page 49, the paragraph beginning on line 15:

Kerogen in region 9 may be treated to generate methane and hydrogen. For example, if such kerogen was previously treated (e.g., it was previously region 7 kerogen), then after pyrolysis, longer hydrocarbon chains of the hydrocarbons may have already cracked and been produced from the formation. Carbon and hydrogen, however, may still be present in the formation.

On page 50, the paragraph beginning on line 5:

Kerogen is composed of organic matter that has been transformed due to a maturation process. Hydrocarbon containing formations that include kerogen may include, but are not limited to, coal ~~containing~~ formations and oil shale ~~containing~~ formations. Examples of hydrocarbon containing formations that may not include kerogen are formations containing heavy hydrocarbons (e.g., tar sands). The maturation process may include two stages: a biochemical stage and a geochemical stage. The biochemical stage typically involves degradation of organic material by both aerobic and anaerobic organisms. The geochemical stage typically involves conversion of organic matter due to temperature changes and significant pressures. During maturation, oil and gas may be produced as the organic matter of the kerogen is transformed.

On page 51, the three paragraphs beginning on line 10:

The dashed lines in FIG. 2 correspond to vitrinite reflectance. The vitrinite reflectance is a measure of maturation. As kerogen undergoes maturation, the composition of the kerogen usually changes. For example, as kerogen undergoes maturation, volatile matter of kerogen tends to decrease. Rank classifications of kerogen indicate the level to which kerogen has matured. For example, as kerogen undergoes maturation, the rank of kerogen increases. Therefore, as rank increases, the volatile matter of kerogen tends to decrease. In addition, the moisture content of kerogen generally decreases as the rank

increases. At higher ranks, however, the moisture content may become relatively constant. For example, higher rank kerogens that have undergone significant maturation, such as semi-anthracite or anthracite coal, tend to have a higher carbon content and a lower volatile matter content than lower rank kerogens such as lignite. For example, rank stages of coal containing formations include the following classifications, which are listed in order of increasing rank and maturity for type III kerogen: wood, peat, lignite, sub-bituminous coal, high volatile bituminous coal, medium volatile bituminous coal, low volatile bituminous coal, semi-anthracite, and anthracite. In addition, as rank increases, kerogen tends to exhibit an increase in aromatic nature.

Hydrocarbon containing formations may be selected for in situ treatment based on properties of at least a portion of the formation. For example, a formation may be selected based on richness, thickness, and depth (i.e., thickness of overburden) of the formation. In addition, a formation may be selected that will have relatively high quality fluids produced from the formation. In certain embodiments the quality of the fluids to be produced may be assessed in advance of treatment, thereby generating significant cost savings since only more optimal formations will be selected for treatment. Properties that may be used to assess hydrocarbons in a formation include, but are not limited to, an amount of hydrocarbon liquids that tend to be produced from the hydrocarbons, a likely API gravity of the produced hydrocarbon liquids, an amount of hydrocarbon gas that tends to be produced from the hydrocarbons, and/or an amount of carbon dioxide and water that tend to be produced from the hydrocarbons.

Another property that may be used to assess the quality of fluids produced from certain kerogen containing formations is vitrinite reflectance. Such formations include, but are not limited to, coal containing formations and oil shale containing formations. Hydrocarbon containing formations that include kerogen can typically be assessed/selected for treatment based on a vitrinite reflectance of the kerogen. Vitrinite reflectance is often related to a hydrogen to carbon atomic ratio of a kerogen and an oxygen to carbon atomic ratio of the kerogen, as shown by the dashed lines in Fig. 2. For example, a van Krevelen diagram may be useful in selecting a resource for an in situ conversion process.

On page 57, the paragraph beginning on line 14:

Dewatering wells 110 may be placed in one or more rings surrounding selected portions of the formation. New dewatering wells may need to be installed as an area being treated by the in situ conversion process expands. An outermost row of dewatering wells may inhibit a significant amount of water from flowing into the portion of formation that is heated or to be heated. Water produced from the outermost row of dewatering wells should be substantially clean, and may require little or no treatment before being released. An innermost row of dewatering wells may inhibit water that bypasses the outermost row from flowing into the portion of formation that is heated or to be heated. The innermost row of dewatering wells may also inhibit outward migration of vapor from a heated portion of the formation into surrounding portions of the formation. Water produced by the innermost row of dewatering wells may include some hydrocarbons. The water may need to be treated before being released. Alternately, water with hydrocarbons may be stored and used to produce synthesis gas from a portion of the formation during a synthesis gas phase of the in situ conversion process. The dewatering wells may reduce heat loss to surrounding portions of the formation, may increase production of vapors from the heated portion, and may inhibit contamination of a water table proximate the heated portion of the formation.

On page 58, the paragraph beginning on line 6:

The hydrocarbons to be treated may be located under a large area. The in situ conversion system may be used to treat small portions of the formation, and other sections of the formation may be treated as time progresses. In an embodiment of a system for treating an oil shale ~~containing~~ formation, a field layout for 24 years of development may be divided into 24 individual plots that represent individual drilling years. Each plot may include 120 "tiles" (repeating matrix patterns) wherein each tile is made of 6 rows by 20 columns. Each tile may include 1 production well and 12 or 18 heater wells. The heater wells may be placed in an equilateral triangle pattern with, for example, a well spacing of about 12 m. Production wells may be located in centers of equilateral triangles of heater wells, or the production wells may be located approximately at a midpoint between two adjacent heater wells.

On page 59, the paragraph beginning on line 15:

In certain embodiments a first portion of a heater well may extend from a surface of the ground, through an overburden, and into a hydrocarbon containing formation. A second portion of the heater well may include one or more heater wells in the hydrocarbon containing formation. The one or more heater wells may be disposed within the hydrocarbon containing formation at various angles. In some embodiments, at least one of the heater wells may be disposed substantially parallel to a boundary of the hydrocarbon containing formation. In alternate embodiments, at least one of the heater wells may be substantially perpendicular to the hydrocarbon containing formation. In addition, one of the one or more heater wells may be positioned at an angle between perpendicular and parallel to a layer in the formation.

On page 63, the two paragraphs beginning on line 8:

In some embodiments, a plurality of heated portions may exist within a unit of heat sources. A unit of heat sources refers to a minimal number of heat sources that form a template that may be repeated to create a pattern of heat sources within the formation. The heat sources may be located within the formation such that superposition (overlapping) of heat produced from the heat sources is effective. For example, as illustrated in FIG. 7, transfer of heat from two or more heat sources 330 results in superposition of heat 332 to be effective within an area defined by the unit of heat sources. Superposition may also be effective within an interior of a region defined by two, three, four, five, six, or more heat sources. For example, an area in which superposition of heat 332 is effective includes an area to which significant heat is transferred by two or more heat sources of the unit of heat sources. An area in which superposition of heat is effective may vary depending upon, for example, the spacings between heat sources.

Superposition of heat may increase a temperature in at least a portion of the formation to a temperature sufficient for pyrolysis of hydrocarbon within the portion. In this manner, superposition of heat 332 tends to increase the amount of hydrocarbons in a formation that may be pyrolyzed. As such, a plurality of areas that are within a pyrolysis temperature range may exist within the unit of heat sources. The selected sections 334 may include areas ~~at~~ in a

pyrolysis temperature range due to heat transfer from only one heat source, as well as areas ~~at~~ in a pyrolysis temperature range due to superposition of heat.

On page 64, the paragraph beginning on line 24:

Because permeability and/or porosity increases in the heated formation, produced vapors may flow considerable distances through the formation with relatively little pressure differential. Therefore, in some embodiments, production wells may be provided near an upper surface of the formation. Increases in permeability may result from a reduction of mass of the heated portion due to vaporization of water, removal of hydrocarbons, and/or creation of fractures. In this manner, fluids may more easily flow through the heated portion.

On page 66, the two paragraphs beginning on line 30:

A distance from a node of a polygon to a centroid of the polygon is smallest for a 3 sided polygon and increases with increasing number of sides of the polygon. The distance from a node to the centroid for an equilateral triangle is $(\text{length}/2)/(\text{square root}(3)/2)$ or 0.5774 times the length. For a square, the distance from a node to the centroid is $(\text{length}/2)/(\text{square root}(2)/2)$ or 0.7071 times the length. For a hexagon, the distance from a node to the centroid is $(\text{length}/2)/(1/2)$ or the length. The difference in distance between a heat source and a mid-point to a second heat sources $(\text{length}/2)$ and the distance from a heat source to the centroid for an equilateral pattern (0.5774 times the length) is significantly less for the equilateral triangle pattern than for any higher order polygon pattern. The small difference means that superposition of heat may develop more rapidly and that the formation between heat sources may rise to a substantially more uniform temperature using an equilateral triangle pattern rather than a higher order polygon pattern.

Triangular patterns tend to provide more uniform heating to a portion of the formation in comparison to other patterns such as squares and/or hexagons. Triangular patterns tend to provide faster heating to a predetermined temperature in comparison to other patterns such as squares and/or hexagons. Triangle patterns may also result in a small volume of the portion that ~~are~~is overheated. A plurality of units of heat sources such as triangular pattern 401 may be arranged substantially adjacent to each other to form a

repetitive pattern of units over an area of the formation. For example, triangular patterns 401 may be arranged substantially adjacent to each other in a repetitive pattern of units by inverting an orientation of adjacent triangles 401. Other patterns of heat sources 400 may also be arranged such that smaller patterns may be disposed adjacent to each other to form larger patterns.

On page 69, the paragraph beginning on line 18:

For certain thinner formations, heating wells may be placed closer to an edge of the formation (e.g., in a staggered line instead of a line placed in the center of the layer) of the formation to increase the amount of hydrocarbons produced per unit of energy input. A portion of input heating energy may heat non-hydrocarbon containing formation, but the staggered pattern may allow superposition of heat to heat a majority of the hydrocarbon formation to pyrolysis temperatures. If the thin formation is heated by placing one or more heater wells in the formation along a center of the thickness, a significant portion of the hydrocarbon containing formation may not be heated to pyrolysis temperatures. In some embodiments, placing heater wells closer to an edge of the formation may increase the volume of formation undergoing pyrolysis per unit of energy input.

On page 78, the paragraph beginning on line 17:

With time, reaction zone 524 may slowly extend radially to greater diameters from opening 514 as hydrocarbons are oxidized. Reaction zone 524 may, in many embodiments, maintain a relatively constant width. For example, reaction zone 524 may extend radially at a rate of less than about 0.91 m per year for a hydrocarbon containing formation. For example, for a ~~coal-containing~~coal formation, reaction zone 524 may extend radially at a rate between about 0.5 m per year to about 1 m per year. For an ~~oil-shale-containing~~oil shale formation, reaction zone 524 may extend radially about 2 m in the first year and at a lower rate in subsequent years due to an increase in volume of reaction zone 524 as reaction zone 524 extends radially. Such a lower rate may be about 1 m per year to about 1.5 m per year. Reaction zone 524 may extend at slower rates for hydrocarbon rich formations (e.g., coal) and at faster rates for formations with more inorganic material in it (e.g., oil shale) since

more hydrocarbons per volume are available for combustion in the hydrocarbon rich formations.

On page 81, the paragraph beginning on line 8:

In certain embodiments one or more natural distributed combustors may be placed along strike and/or horizontally. Doing so tends to reduce pressure differentials along the heated length of the well. The absence of pressure differentials may make controlling the temperature generated along a length of the heater more uniform and ~~more easy~~easier to control.

On page 87, the paragraph beginning on line 16:

In certain embodiments, insulated conductor heaters may be placed in wellbores without support members and/or centralizers. This can be accomplished for heaters if the insulated conductor has a suitable combination of temperature and corrosion resistance, creep strength, length, thickness (diameter) and metallurgy that will inhibit failure of the insulated conductor during use. In an embodiment, insulated conductors that are heated to a working temperature of about 700 °C are less than about 150 meters in length, are made of 310 stainless steel, and may be used without support members.

On page 100, the paragraph beginning on line 18:

In an embodiment, a control system may be configured to control electrical power supplied to an insulated conductor heater. Power supplied to the insulated conductor heater may be controlled with any appropriate type of controller. For alternating current, the controller may, for example, be a tapped transformer. Alternatively, the controller may be a zero crossover electrical heater firing SCR (silicon controlled rectifier) controller. Zero crossover electrical heater firing control may be achieved by allowing full supply voltage to the insulated conductor heater to pass through the insulated conductor heater for a specific number of cycles, starting at the "crossover," where an instantaneous voltage may be zero, continuing for a specific number of complete cycles, and discontinuing when the instantaneous voltage again may cross zero. A specific number of cycles may be blocked, allowing control of the heat output by the insulated conductor heater. For example, the

control system may be arranged to block fifteen and/or twenty cycles out of each sixty cycles that may be supplied by a standard 60 Hz alternating current power supply. Zero crossover firing control may be advantageously used with materials having a low temperature coefficient materials. Zero crossover firing control may substantially inhibit current spikes from occurring in an insulated conductor heater.

On page 101, the paragraph beginning on line 23:

Conductor 580 may be centered in conduit 582 through centralizer 581. Centralizer 581 may electrically isolate conductor 580 from conduit 582. In addition, centralizer 581 may be configured to locate conductor 580 within conduit 582. Centralizer 581 may be made of a ceramic material or a combination of ceramic and metallic materials. More than one centralizer 581 may be configured to substantially inhibit deformation of conductor 580 in conduit 582 during use. More than one centralizer 581 may be spaced at intervals between approximately 0.5 m and approximately 3 m along conductor 580. Centralizer 581 may be made of ceramic, 304 stainless steel, 310 stainless steel, or other types of metal. Centralizer 581 may be configured as shown in FIG. 22 and/or FIGSs. 23a and 23b.

On page 102, the paragraph beginning on line 2:

As depicted in FIG. 20, sliding connector 583 may couple an end of conductor 580 disposed proximate a lowermost surface of conduit 582. Sliding connector 583 allows for differential thermal expansion between conductor 580 and conduit 582. Sliding connector 583 is attached to a conductor 580 located at the bottom of the well at a low resistance section 584 which may have a greater cross-sectional area. The lower resistance of section 584 allows the sliding connector to operate at temperatures no greater than about 90 °C. In this manner, corrosion of the sliding connector components is minimized and therefore contact resistance between sliding connector 583 and conduit 582 is also minimized. Sliding connector 583 may be configured as shown in FIG. 20 and as described in any of the embodiments herein. The substantially low resistance section 584 of the conductor 580 may couple conductor 580 to wellhead 690 as depicted in FIG. 19. Wellhead 690 may be configured as shown in FIG. 21 and as described in any of the embodiments herein. As depicted in FIG. 19, ~~E~~lectrical current may be applied to conductor 580 from power cable

585 through a low resistance section 584 of the conductor 580. Electrical current may pass from conductor 580 through sliding connector 583 to conduit 582. Conduit 582 may be electrically insulated from overburden casing 541 and from wellhead 690 to return electrical current to power cable 585. Heat may be generated in conductor 580 and conduit 582. The generated heat may radiate within conduit 582 and opening 514 to heat at least a portion of formation 516. As an example, a voltage of about 330 volts and a current of about 795 amps may be supplied to conductor 580 and conduit 582 in a 229 m (750 ft) heated section to generate about 1150 watts/meter of conductor 580 and conduit 582.

On page 111, the paragraph beginning on line 24:

An elongated member may have a length of about 650 meters. Longer lengths may be achieved using sections of high strength alloys, but such elongated members may be expensive. In some embodiments, an elongated member may be supported by a plate in a wellhead. The elongated member may include sections of different conductive materials that are welded together end-to-end. A large amount of electrically conductive weld material may be used to couple the separate sections together to increase strength of the resulting member and to provide a path for electricity to flow that will not result in arcing and/or corrosion at the welded connections. The different conductive materials may include alloys with a high creep resistance. The sections of different conductive materials may have varying diameters to ensure uniform heating along the elongated member. A first metal that has a higher creep resistance than a second metal typically has a higher resistivity than the second metal. The difference in resistivities may allow a section of larger cross sectional area, more creep resistant, first metal to dissipate the same amount of heat as a section of smaller cross sectional area, second metal. The cross sectional areas of the two different metals may be tailored to result in substantially the same amount of heat dissipation in two welded together sections of the metals. The conductive materials may include, but are not limited to, 617 Inconel, HR-120, 316 stainless steel, and 304 stainless steel. For example, an elongated member may have a 60 meter section of 617 Inconel, 60 meter section of HR-120, and 150 meter section of 304 stainless steel. In addition, the elongated member may have a low resistance section that may run from the wellhead through the overburden. This low resistance section may decrease the heating within the formation from the wellhead through

the overburden. The low resistance section may be the result of, for example, choosing a substantially electrically conductive material and/or increasing the cross-sectional area available for electrical conduction.

On page 118, the paragraph beginning on line 4:

Inner conduit 612 may be configured to provide oxidation products 613 into outer conduit 615 proximate a bottom of opening 614. Inner conduit 612 may have insulation 612a. FIG. 27 illustrates an embodiment of inner conduit 612 with insulation 612a and ceramic insulator 612b disposed on an inner surface of inner conduit 612. Insulation 612a may be configured to substantially inhibit heat transfer between fluids in inner conduit 612 and fluids in outer conduit 615. A thickness of insulation 612a may be varied along a length of inner conduit 612 such that heat transfer to formation 516 may vary along the length of inner conduit 612. For example, a thickness of insulation 612a may be tapered to from a larger thickness to a lesser thickness from a top portion to a bottom portion, respectively, of inner conduit 612 in opening 614. Such a tapered thickness may provide substantially more uniform heating of formation 516 along the length of inner conduit 612 in opening 614. Insulation 612a may include ceramic and metal materials. Oxidation products 613 may return to surface 550 through outer conduit 615. Outer conduit may have insulation 615a as depicted in FIG. 26. Insulation 615a may be configured to substantially inhibit heat transfer from outer conduit 615 to overburden 540.

On page 124, the paragraph beginning on line 13:

It is to be understood that the above equations can be used to assess or estimate temperatures, average temperatures (e.g., over selected sections of the formation), heat input, etc. Such equations do not take into account other factors (such as heat losses) ~~which~~, which would also have some effect on heating and temperatures assessments. However such factors can ordinarily be addressed with correction factors, as is commonly done in the art.

On pages 134 to 135, Tables 1a and 1b:

TABLE 1a

PROPERTY	A_1a_1	A_2a_2	a_3	a_4
API Gravity	-0.738549	-8.893902	4752.182	-145484.6
Ethene/Ethane Ratio	-15543409	3261335	-303588.8	-2767.469
Weight Percent of Hydrocarbons Having a Carbon Number Greater Than 25	0.1621956	-8.85952	547.9571	-24684.9
Atomic H/C Ratio	2950062	-16982456	32584767	-20846821
Liquid Production (gal/ton)	119.2978	-5972.91	96989	-524689
Equivalent Liquid Production (gal/ton)	-6.24976	212.9383	-777.217	-39353.47
% Fischer Assay	0.5026013	-126.592	9813.139	-252736

TABLE 1b

PROPERTY	b_1	b_2	b_3	B_4b_4
API Gravity	0.003843	-0.279424	3.391071	96.67251
Ethene/Ethane Ratio	-8974.317	2593.058	-40.78874	23.31395
Weight Percent of Hydrocarbons Having a Carbon Number Greater Than 25	-0.0005022	0.026258	-1.12695	44.49521
Atomic H/C Ratio	790.0532	-4199.454	7328.572	-4156.599
Liquid Production (gal/ton)	-0.17808	8.914098	-144.999	793.2477
Equivalent Liquid Production (gal/ton)	-0.03387	2.778804	-72.6457	650.7211
% Fischer Assay	-0.0007901	0.196296	-15.1369	395.3574

On page 141, the paragraph beginning on line 16:

In some embodiments, the non-condensable hydrocarbons may include, but are not limited to, hydrocarbons having less than about 5 carbon atoms, H₂, CO₂, ammonia, H₂S, N₂ and/or CO. In certain embodiments, non-condensable hydrocarbons of a fluid produced from a portion of a hydrocarbon containing formation may have a weight ratio of hydrocarbons

having carbon numbers from 2 through 4 (“C₂₋₄” hydrocarbons) to methane of greater than about 0.3, greater than about 0.75, or greater than about 1 in some circumstances. For example, non-condensable hydrocarbons of a fluid produced from a portion of an oil shale or heavy hydrocarbon containing formation may have a weight ratio of hydrocarbons having carbon numbers from 2 through 4, to methane, of greater than approximately 1. In addition, non-condensable hydrocarbons of a fluid produced from a portion of a ~~coal~~-containing coal formation may have a weight ratio of hydrocarbons having carbon numbers from 2 through 4, to methane, of greater than approximately 0.3.

On page 142, the paragraph beginning on line 23:

The non-condensable hydrocarbons of fluid produced from a hydrocarbon containing formation may have a H₂ content of greater than about 5 % by weight, greater than about 10 % by weight, or even greater than about 15 % by weight. The H₂ may be used, for example, as a fuel for a fuel cell, to hydrogenate hydrocarbon fluids in situ, and/or to hydrogenate hydrocarbon fluids ex situ. In addition, presence of H₂ within a formation fluid in a heated section of a hydrocarbon containing formation is believed to increase the quality of produced fluids. In certain embodiments, the hydrogen to carbon atomic ratio of a produced fluid may be at least approximately 1.7 or above. For example, the hydrogen to carbon atomic ratio of a produced fluid may be approximately 1.8, approximately 1.9, or greater.

On page 144, the paragraph beginning on line 4:

In certain embodiments, a fluid produced from a formation (e.g., a ~~coal~~-containing coal formation) may include oxygenated hydrocarbons. For example, condensable hydrocarbons of the produced fluid may include an amount of oxygenated hydrocarbons greater than about 5 % by weight of the condensable hydrocarbons. Alternatively, the condensable hydrocarbons may include an amount of oxygenated hydrocarbons greater than about 1.0 % by weight of the condensable hydrocarbons. Furthermore, the condensable hydrocarbons may include an amount of oxygenated hydrocarbons greater than about 1.5 % by weight of the condensable hydrocarbons or greater than about 2.0 % by weight of the condensable hydrocarbons. In an embodiment, the oxygenated hydrocarbons may include, but are not limited to, phenol and/or substituted phenols. In some embodiments, phenol and

substituted phenols may have more economic value than other products produced from an in situ conversion process. Therefore, an in situ conversion process may be utilized to produce phenol and/or substituted phenols. For example, generation of phenol and/or substituted phenols may increase when a fluid pressure within the formation is maintained at a lower pressure.

On page 146, the paragraph beginning on line 15:

In certain embodiments, the condensable hydrocarbons of a fluid produced from a formation may include compounds containing oxygen. For example, in certain embodiments (e.g., for oil shale and heavy hydrocarbons) less than about 1 % by weight (when calculated on an elemental basis) of the condensable hydrocarbons may be oxygen containing compounds (e.g., typically the oxygen may be in oxygen containing compounds such as phenol, substituted phenols, ketones, etc.). In certain other embodiments, (e.g., for ~~coal~~ coal containing coal formations) between about 5 % by weight and about 30 % by weight of the condensable hydrocarbons may typically include oxygen containing compounds such as phenols, substituted phenols, ketones, etc. In some instances, certain compounds containing oxygen (e.g., phenols) may be valuable and, as such, may be economically separated from the produced fluid.

On page 149, the paragraph beginning on line 30:

Thermal diffusivity within a hydrocarbon containing formation may vary depending on, for example, a density of the hydrocarbon containing formation, a heat capacity of the formation, and a thermal conductivity of the formation. As pyrolysis occurs within a selected section, the hydrocarbon containing ~~formation~~ mass may be removed from the selected section. The removal of mass may include, but is not limited to, removal of water and a transformation of hydrocarbons to formation fluids. For example, a lower thermal conductivity may be expected as water is removed from a ~~coal~~ coal containing coal formation. This effect may vary significantly at different depths. At greater depths a lithostatic pressure may be higher, and may close certain openings (e.g., cleats and/or fractures) in the coal. The closure of the coal openings may increase a thermal conductivity of the coal. In some

embodiments, a higher thermal conductivity may be observed due to a higher lithostatic pressure.

On page 152, the paragraph beginning on line 15:

Substantially uniform heating of the hydrocarbon containing formation may result in a substantially uniform increase in permeability. For example, uniformly heating may generate a series of substantially uniform fractures within the heated portion due to thermal stresses generated in the formation. Heating substantially uniformly may generate pyrolysis fluids from the portion in a substantially homogeneous manner. Water removed due to vaporization and production may result in increased permeability of the heated portion. In addition to creating fractures due to thermal stresses, fractures may also be generated due to fluid pressure increase. As fluids are generated within the heated portion, a fluid pressure within the heated portion may also increase. As the fluid pressure approaches a lithostatic pressure of the heated portion, fractures may be generated. Substantially uniform heating and homogeneous generation of fluids may generate substantially uniform fractures within the heated portion. In some embodiments, a permeability of a heated section of a hydrocarbon containing formation may not vary by more than a factor of about 10.

On page 156, the paragraph beginning on line 24:

Synthesis gas may be produced from a dipping formation from wells used during pyrolysis of the formation. As shown in FIG. 4, synthesis gas production wells 206 may be located above and down dip from an injection well 208202. Hot synthesis gas producing fluid may be introduced into injection well 208202. Hot synthesis gas fluid that moves down dip may generate synthesis gas that is produced through synthesis gas production wells 206. Synthesis gas generating fluid that moves up dip may generate synthesis gas in a portion of the formation that is at synthesis gas generating temperatures. A portion of the synthesis gas generating fluid and generated synthesis gas that moves up dip above the portion of the formation at synthesis gas generating temperatures may heat adjacent portions of the formation. The synthesis gas generating fluid that moves up dip may condense, heat adjacent portions of formation, and flow downwards towards or into a portion of the formation at

synthesis gas generating temperature. The synthesis gas generating fluid may then generate additional synthesis gas.

On page 163, the paragraph beginning on line 26:

The first temperature may be substantially different than the second temperature. Alternatively, the first and second temperatures may be approximately the same temperature. For example, a temperature sufficient to allow generation of synthesis gas having different compositions may vary depending on compositions of the first and second portions and/or prior pyrolysis of hydrocarbons within the first and second portions. The first synthesis gas generating fluid may have substantially the same composition as the second synthesis gas generating fluid. Alternatively, the first synthesis gas generating fluid may have a different composition than the second synthesis gas generating fluid. Appropriate first and second synthesis gas generating fluids may vary depending upon, for example, temperatures of the first and second portions, compositions of the first and second portions, and prior pyrolysis of hydrocarbons within the first and second portions.

On page 166, the paragraph beginning on line 2:

FIG. 33 illustrates a reduced emission energy process. Carbon dioxide 928 produced by energy generation unit 902 may be separated from fluids exiting the energy generation unit. Carbon dioxide may be separated from H_2 at high temperatures by using a hot palladium film supported on porous stainless steel or a ceramic substrate, or high temperature pressure swing adsorption. The carbon dioxide may be sequestered in spent hydrocarbon containing formation 922, injected into oil producing fields 924 for enhanced oil recovery by improving mobility and production of oil in such fields, sequestered into a deep hydrocarbon containing formation 926 containing methane by adsorption and subsequent desorption of methane, or re-injected 928 into a section of the formation through a synthesis gas production well to produce carbon monoxide. Carbon dioxide leaving the energy generation unit may be sequestered in a dewatered coal bed methane reservoir. The water for synthesis gas generation may come from dewatering a coal bed methane reservoir. Additional methane can also be produced by alternating carbon dioxide and nitrogen. An example of a method for sequestering carbon dioxide is illustrated in U.S. Pat. No. 5,566,756 to Chaback et al.,

which is incorporated by reference as if fully set forth herein. Additional energy may be utilized by removing heat from the carbon dioxide stream leaving the energy generation unit.

On page 166, the paragraph beginning on line 27:

In one embodiment, a spent hydrocarbon containing formation may be mined. The mined material may in some embodiments be used for metallurgical purposes such as a fuel for generating high temperatures during production of steel. Pyrolysis of a coal containing coal formation may substantially increase a rank of the coal. After pyrolysis, the coal may be substantially transformed to a coal having characteristics of anthracite. A spent hydrocarbon containing formation may have a thickness of 30 m or more. Anthracite coal seams, which are typically mined for metallurgical uses, may be only about one meter in thickness.

On page 178, the paragraph beginning on line 4:

Ammonia and urea may be produced using a carbon containing formation, and using an O₂ rich stream and an N₂ rich stream. The O₂ rich stream and synthesis gas generating fluid may be provided to a formation. The formation may be heated, or partially heated, by oxidation of carbon in the formation with the O₂ rich stream. H₂ in the synthesis gas, and N₂ from the N₂ rich stream, may be provided to an ammonia synthesis process to generate ammonia.

On page 179, the paragraph beginning on line 22:

FIG. 43 illustrates an embodiment of a method for preparing a nitrogen stream for an ammonia and urea process. Air 2060 may be injected into hot carbon containing formation 2062 to produce carbon dioxide by oxidation of carbon in the formation. In an embodiment, a heater may be configured to heat at least a portion of the carbon containing formation to a temperature sufficient to support oxidation of the carbon. The temperature sufficient to support oxidation may be, for example, about 260 °C for coal. Stream 2064 exiting the hot formation may be composed substantially of carbon dioxide and nitrogen. Nitrogen may be separated from carbon dioxide by passing the stream through cold spent carbon containing formation 2066. Carbon dioxide may be preferentially adsorbed versus nitrogen in the cold

spent formation 2066. For example, at 50 °C and 0.35 bars, the adsorption of carbon dioxide on a spent portion of coal may be about 72 m³/metric ton compared to about 15.4 m³/metric ton for nitrogen. Nitrogen 2068 exiting the cold spent portion 2066 may be supplied to ammonia production facility 2070 with H₂ stream 2072 to produce ammonia 2074. The H₂ stream may be obtained by methods disclosed herein, for example, the methods described in FIGS. 41 and 42.

On page 188, the paragraph beginning on line 25:

FIG. 50 illustrates an alternate embodiment of pattern 2406 of heat sources 2400 that may be arranged in a “7 spot” pattern with production well 2402. In the “7 spot” pattern, six heat sources 2400 may be arranged substantially equidistant from production well 2402 and substantially equidistant from each other as depicted in FIG. 50. Heat sources 2400 may also be configured as a production well. Also, production well 2402 may be configured as a heat source. A spacing between heat sources 2400 and production well 2402 may be determined as described in any of the above embodiments.

On page 191, the paragraph beginning on line 8:

In an embodiment, condensable hydrocarbons of a fluid produced from a relatively permeable formation may include aromatic compounds. For example, greater than about 20 % by weight of the condensable hydrocarbons may include aromatic compounds. In another embodiment, an aromatic compound weight percent may include greater than about 30 % of the condensable hydrocarbons. The condensable hydrocarbons may also include di-aromatic compounds. For example, less than about 20 % by weight of the condensable hydrocarbons may include di-aromatic compounds. In another embodiment, di-aromatic compounds may include less than about 15 % by weight of the condensable hydrocarbons. The condensable hydrocarbons may also include tri-aromatic compounds. For example, less than about 4 % by weight of the condensable hydrocarbons may include tri-aromatic compounds. In another embodiment, ~~tri-aromatic compounds may include less than about 1 % by weight of the~~ condensable hydrocarbons may include tri-aromatic compounds.

On page 196, the paragraph beginning on line 29:

FIG. 53 is a view of an embodiment of a heat source and production well pattern illustrating a pyrolysis zone and a low viscosity zone. Heat sources 2512 along plane 2504 and plane 2506 may heat planar region 2508 to create a pyrolysis zone. Heating may create thermal fractures 2510 in the pyrolysis zone. Heating with heat sources 2514 in planes 2516, 2518, 2520, and 2522 may create a low viscosity zone with an increased permeability due to thermal fractures. Pressure differential between the low viscosity zone and the pyrolysis zone may force mobilized fluid from the low viscosity zone into the pyrolysis zone. The permeability created by thermal fractures 2510 may be sufficiently high to create a substantially uniform pyrolysis zone. Pyrolyzation fluids may be produced through production well 2500.

On page 202, the paragraph beginning on line 9:

FIGS. 62, 63, 64, and 65 illustrate alternate embodiments in which both production wells and heat sources may be located at the apices of a triangular grid. In FIG. 62, a triangular grid, with a spacing of s , may have production wells 2701 spaced at a distance of $2s$. A hexagonal pattern may include one ring 2730 of six heat sources 2732. Each heat source 2732 may provide substantially equal amounts of heat to two production wells 2701. Therefore, each ring 2730 of six heat sources 2732 contributes approximately three equivalent heat sources per production well 2701.

On page 211, the paragraph beginning on line 2:

FIG. 73 illustrates an embodiment of an additional processing unit that may be included in surface facilities 2800 such as the facilities depicted in FIG. 71. Air 2903 may be fed to air separation unit 2900. Air separation unit 2900 may be configured to generate nitrogen stream 2902 and oxygen stream 2905. Oxygen stream 2905 and steam 2904 may be injected into exhausted coal resource 2906 to generate synthesis gas 2907. Produced synthesis gas 2907 may be provided to Shell Middle Distillates process unit 2910 that may be configured to produce middle distillates 2912. In addition, produced synthesis gas 2907 may be provided to catalytic methanation process unit 2914 that may be configured to produce natural gas 2916. Produced synthesis gas 2907 may also be provided to methanol production unit 2918 to produce methanol 2920. Furthermore, produced synthesis gas 2907 may be

provided to process unit 2922 for production of ammonia and/or urea 2924, and fuel cell 2926 that may be configured to produce electricity 2928. Synthesis gas 2907 may also be routed to power generation unit 2930, such as a turbine or combustor, to produce electricity 2932.

On page 213, the paragraph beginning on line 16:

FIG. 78 illustrates temperature profile 3110 after three years of heating for a triangular pattern with a 12.2 m spacing in a typical Green River oil shale. The triangular pattern may be configured as shown in FIG. 76. Temperature profile 3110 is a three-dimensional plot of temperature versus a location within a triangular pattern. FIG. 79 illustrates temperature profile 3108 after three years of heating for a square pattern with 11.3 m spacing in a typical Green River oil shale. Temperature profile 3108 is a three-dimensional plot of temperature versus a location within a square pattern. The square pattern may be configured as shown in FIG. 76a. FIG. 79a illustrates temperature profile 3109 after three years of heating for a hexagonal pattern with 10.0 m spacing in a typical Green River oil shale. Temperature profile 3109 is a three-dimensional plot of temperature versus a location within a hexagonal pattern. The hexagonal pattern may be configured as shown in FIG. 77.

On page 215, the paragraph beginning on line 2:

FIG. 81 illustrates a comparison plot between the average pattern temperature 3120 (in degrees Celsius), ~~3120~~ temperatures at coldest spot 3118 for triangular patterns, coldest spot 3114 for hexagonal patterns, point 3116 located at the center of a side of triangular pattern midway between heaters, and point 3112 located at the center of a side of hexagonal pattern midway between heaters, as a function of time (in years). FIG. 81a illustrates a comparison plot between the average pattern temperature 3120 (in degrees Celsius), temperatures at coldest spot 3117 and point 3119 located at the center of a side of a pattern midway between heaters, as a function of time (in years), for a square pattern.

On page 216, the paragraph beginning on line 29:

A spacing of heat sources in a triangular pattern, which may yield the same process time as a hexagonal pattern having about a 10.0 m space between heat sources, may be equal to approximately 14.3 m. In this manner, the total process time of a ~~hexagonal~~ triangular pattern may be achieved by using about 26 % less heat sources than may be included in such a hexagonal pattern. In this manner, such a triangular pattern may have substantially lower capital and operating costs. As such, this triangular pattern may also be more economical than a hexagonal pattern.

On page 225, the four paragraphs beginning on line 24:

FIG. 91 illustrates oil quality produced from an ~~oil shale containing~~ oil shale formation as a function of pressure and temperature. Lines indicating different oil qualities, as defined by API gravity, are plotted. For example, the quality of the produced oil was 45° API when pressure was maintained at about 6 bars absolute and a temperature was about 375 °C. As described in above embodiments, low pyrolysis temperatures and relatively high pressures may produce a high API gravity oil.

FIG. 92 illustrates an ethene to ethane ratio produced from an ~~oil shale containing~~ oil shale formation as a function of pressure and temperature. For example, at a pressure of 11.2 bars absolute and a temperature of 375 °C, the ratio of ethene to ethane is approximately 0.01. The volume ratio of ethene to ethane may predict an olefin to alkane ratio of hydrocarbons produced during pyrolysis. To control olefin content, operating at lower pyrolysis temperatures and a higher pressure may be beneficial. Olefin content in above described embodiments may be reduced by operating at low pyrolysis temperature and a high pressure.

FIG. 93 depicts the dependence of yield of equivalent liquids produced from an ~~oil shale containing~~ oil shale formation as a function of temperature and pressure. Line 3340 represents the pressure-temperature combination at which $8.38 \times 10^{-5} \text{ m}^3$ of fluid per kilogram of oil shale (20 gallons/ton). The pressure/temperature plot results in a line 3342 for the production of total fluids per ton of oil shale equal to $1.05 \times 10^{-5} \text{ m}^3/\text{kg}$ (25 gallons/ton). Line 3344 illustrates that $1.21 \times 10^{-4} \text{ m}^3$ of fluid is produced from 1 kilogram of

oil shale (30 gallons/ton). For example, at a temperature of about 325 °C and a pressure of about 8 bars absolute the resulting equivalent liquids was $8.38 \times 10^{-5} \text{ m}^3/\text{kg}$. As temperature of the retort increased and the pressure decreased the yield of the equivalent liquids produced increased. Equivalent liquids produced was defined as the amount of liquid equivalent to the energy value of the produced gas and liquids.

FIG. 94 illustrates a plot of oil yield produced from treating an ~~oil shale containing~~oil shale formation, measured as volume of liquids per ton of the formation, as a function of temperature and pressure of the retort. Temperature is illustrated in units of Celsius on the x-axis, and pressure is illustrated in units of bars absolute on the y-axis. As shown in FIG. 94, the yield of liquid/condensable products increases as temperature of the retort increases and pressure of the retort decreases. The lines on FIG. 94 correspond to different liquid production rates measured as the volume of liquids produced per weight of oil shale and are shown in Table 3.

On page 227, the three paragraphs beginning on line 2:

FIG. 95 illustrates yield of oil produced from treating an ~~oil shale containing~~oil shale formation expressed as a percent of Fischer assay as a function of temperature and pressure. Temperature is illustrated in units of degrees Celsius on the x-axis, and gauge pressure is illustrated in units of bars on the y-axis. Fischer assay was used as a method for assessing a recovery of hydrocarbon condensate from the oil shale. In this case, a maximum recovery would be 100% of the Fischer assay. As the temperature decreased and the pressure increased, the percent of Fischer assay yield decreased.

FIG. 96 illustrates hydrogen to carbon ratio of hydrocarbon condensate produced from an ~~oil shale containing~~oil shale formation as a function of a temperature and pressure. Temperature is illustrated in units of degrees Celsius on the x-axis, and pressure is illustrated in units of bars on the y-axis. As shown in FIG. 96, a hydrogen to carbon ratio of hydrocarbon condensate produced from an ~~oil shale containing~~oil shale formation decreases as a temperature increases and as a pressure decreases. As described in more detail with respect to other embodiments herein, treating an ~~oil shale containing~~oil shale formation at

high temperatures may decrease a hydrogen concentration of the produced hydrocarbon condensate.

FIG. 97 illustrates the effect of pressure and temperature within an ~~oil shale~~ oil shale formation on a ratio of olefins to paraffins. The relationship of the value of one of the properties (R) with temperature has the same functional form as the pressure-temperature relationships previously discussed. In this case the property (R) can be explicitly expressed as a function of pressure and temperature.

$$R = \exp[F(P)/T + G(P)]$$

$$F(p) = f_1*(P)^3 + f_2*(P)^2 + f_3*(P) + f_4$$

$$G(p) = g_1*(P)^3 + g_2*(P)^2 + g_3*(P) + g_4$$

wherein R a value of the property, T is the absolute temperature (in degrees Kelvin), $F(P)$ and $G(P)$ are functions of pressure representing the slope and intercept of a plot of R versus $1/T$.

On page 228, the two paragraphs beginning on line 23:

FIG. 98 illustrates a relationship between an API gravity of a hydrocarbon condensate fluid, the partial pressure of molecular hydrogen within the fluid, and a temperature within an ~~oil shale~~ oil shale formation. As illustrated in FIG. 98, as a partial pressure of hydrogen within the fluid increased, the API gravity generally increased. In addition, lower pyrolysis temperatures appear to have increased the API gravity of the produced fluids. Maintaining a partial pressure of molecular hydrogen within a heated portion of a hydrocarbon containing formation may increase the API gravity of the produced fluids.

In FIG. 99, a quantity of oil liquids produced in m^3 of liquids per kg of ~~oil shale~~ oil shale formation is plotted versus a partial pressure of H_2 . Also illustrated in FIG. 99 are various curves for pyrolysis occurring at different temperatures. At higher pyrolysis temperatures production of oil liquids was higher than at the lower pyrolysis temperatures. In addition, high pressures tended to decrease the quantity of oil liquids

produced from an ~~oil shale containing~~oil shale formation. Operating an in situ conversion process at low pressures and high temperatures may produce a higher quantity of oil liquids than operating at low temperatures and high pressures.

On page 229, the paragraph beginning on line 24:

As illustrated in FIG. 104, the field experiment consisted of a single unconfined hexagonal seven spot pattern on eight foot spacing. Six heat injection wells 3600, drilled to a depth of 40 m, contained 17 m long heating elements that injected thermal energy into the formation from 21 m to 39 m. A single producer well 3602 in the center of the pattern captured the liquids and vapors from the in-situ retort. Three observation wells 3603 inside the pattern and one outside the pattern recorded formation temperatures and pressures. Six dewatering wells 3604 surrounded the pattern on 6 m spacing and were completed in an active aquifer below the heated interval (from 44 m to 61 m). FIG. 105 is a cross-sectional view of the field experiment. A producer well 3602 includes pump 3614. ~~The A~~ lower portion 3612 of producer well 3602 was packed with gravel. ~~The An~~ upper portion 3610 of producer well 3602 was cemented. Heater well 3600 was located a distance of approximately 2.4 meters from producer well 3602. A heating element was located within the heater well and the heater well was cemented in place. Dewatering wells 3604 were located approximately 4.0 meters from heater wells 3600. Coring well 3606 was located approximately 0.5 m from heater wells 3600.

On page 230, the paragraph beginning on line 29:

FIG. 106 illustrates a plot of the maximum temperatures within each of the three inner-most observation wells 3603 (see FIG. 104) versus time. The temperature profiles were very similar for the three observation wells. Heat was provided to the ~~oil shale containing~~oil shale formation for 216 days. As illustrated in FIG. 106, the temperature at the observer wells increased steadily until the heat was turned off.

On page 231, the paragraph beginning on line 20:

As illustrated in FIG. 107, pressure within the ~~oil shale containing~~oil shale material showed some variations initially at different depths, however over time these variations

equalized. FIG. 107 depicts the gauge fluid pressure in the observation well 3603 versus time measured in days at a radial distance of 2.1 m from the production well 3602. The fluid pressures were monitored at depths of 24 m and 33 m. These depths corresponded to a richness within the ~~oil shale containing~~oil shale material of $8.3 \times 10^{-5} \text{ m}^3$ of oil / kg of oil shale at 24 m and $1.7 \times 10^{-4} \text{ m}^3$ of oil / kg of oil shale at 33 m. The higher pressures initially observed at 33 m may be the result of a higher generation of fluids due to the richness of the ~~oil shale containing~~oil shale material at that depth. In addition, at lower depths a lithostatic pressure may be higher, causing the ~~oil shale containing~~oil shale material at 33 m to fracture at higher pressure than at 24 m. During the course of the experiment, pressures within the ~~oil shale containing~~oil shale formation equalized. The equalization of the pressure may have resulted from fractures forming within the ~~oil shale containing~~oil shale formation.

On page 233, the paragraph beginning on line 22:

Experimental data from studies conducted by Lawrence Livermore National Laboratories (LLNL) was plotted along with laboratory data from the in situ conversion process (ICP) for an ~~oil shale containing~~oil shale formation at atmospheric pressure in FIG. 113. The oil recovery as a percent of Fischer assay was plotted against a log of the heating rate. Data from LLNL 3642 included data derived from pyrolyzing powdered oil shale at atmospheric pressure and in a range from about 2 bars absolute to about 2.5 bars absolute. As illustrated in FIG. 113, the data from LLNL 3642 has a linear trend. Data from the ICP 3640 demonstrates that oil recovery, as measured by Fischer assay, was much higher for ICP than the data from LLNL would suggest 3642. FIG. 113 demonstrates that oil recovery from oil shale increases along an S-curve.

On page 234, the paragraph beginning on line 14:

A series of experiments was conducted to determine the effects of various properties of hydrocarbon containing formations on properties of fluids produced from ~~coal containing~~coal formations. The fluids may be produced according to any of the embodiments as described herein. The series of experiments included organic petrography, proximate/ultimate analyses, Rock-Eval pyrolysis, Leco Total Organic Carbon ("TOC"), Fischer Assay, and pyrolysis-gas chromatography. Such a combination of petrographic and

chemical techniques may provide a quick and inexpensive method for determining physical and chemical properties of coal and for providing a comprehensive understanding of the effect of geochemical parameters on potential oil and gas production from coal pyrolysis. The series of experiments were conducted on forty-five cubes of coal to determine source rock properties of each coal and to assess potential oil and gas production from each coal.

On page 236, the three paragraphs beginning on line 23:

Results were also displayed as a yield of products. FIG. 121-124 illustrate the yields of components in terms of m^3 of product per kg of hydrocarbon containing formation, when measured on a dry, ash free basis. As illustrated in FIG. 121 the yield of paraffins increased as the vitrinite reflectance of the coal increased. However, for coals with a vitrinite reflectance greater than about 0.7 to 0.8% the yield of paraffins fell off dramatically. In addition, a yield of cycloalkanes followed similar trends as the paraffins, increasing as the vitrinite reflectance of coal increased and decreasing for coals with a vitrinite reflectance greater than about 0.7% or 0.8% as illustrated in FIG. 122. FIG. 123 illustrates the increase of both paraffins and cycloalkanes as the vitrinite reflectance of coal increases to about 0.7% or 0.8%. As illustrated in FIG. 124, the yield of phenols may be relatively low for coal containing coal material with a vitrinite reflectance of less than about 0.3% and greater than about 1.25%. Production of phenols may be desired due to the value of phenol as a feedstock for chemical synthesis.

As demonstrated in FIG. 125, the API gravity appears to increase significantly when the vitrinite reflectance is greater than about 0.4%. FIG. 126 illustrates the relationship between coal rank, (i.e., vitrinite reflectance), and a yield of condensable hydrocarbons (in gallons per ton on a dry ash free basis) from a coal-containing coal formation. The yield in this experiment appears to be in an optimal range when the coal has a vitrinite reflectance greater than about 0.4% to less than about 1.3%.

FIG. 127 illustrates a plot of CO_2 yield of coal having various vitrinite reflectances. In FIGS. 127 and 128, CO_2 yield is set forth in weight percent on a dry ash free basis. As shown in FIG. 127, at least some CO_2 was released from all of the coal samples. Such CO_2

production may correspond to various oxygenated functional groups present in the initial coal samples. A yield of CO₂ produced from low-rank coal samples was significantly higher than a production from high-rank coal samples. Low-rank coals may include lignite and sub-bituminous brown coals. High-rank coals may include semi-anthracite and anthracite coal. FIG. 128 illustrates a plot of CO₂ yield from a portion of a ~~coal-containing~~ coal formation versus the atomic O/C ratio within a portion of a ~~coal-containing~~ coal formation. As O/C atomic ratio increases, a CO₂ yield increases.

On page 241, the paragraph beginning on line 14:

As shown in FIG. 131, methane started to be produced at temperatures at or above about 270 °C. Since the experiments were conducted at atmospheric pressure, it is believed that the methane is produced from the pyrolysis, and not from mere desorption. Between about 270 °C and about 400 °C, condensable hydrocarbons, methane and H₂ were produced as shown in FIGS. 131, 132, and 133. FIG. 131 shows that above a temperature of about 400 °C methane and H₂ continue to be produced. Above about 450 °C, however, methane concentration decreased in the produced gases whereas the produced gases contained increased amounts of H₂. If heating ~~was~~ were continued, eventually all H₂ remaining in the coal would be depleted, and production of gas from the coal would cease. FIGS. 131-133 indicate that the ratio of a yield of gas to a yield of condensable hydrocarbons will increase as the temperature increases above about 390°C.

On page 242, the paragraph beginning on line 5:

An experiment was conducted to determine an effect of heating on thermal conductivity and thermal diffusivity of a portion of a ~~coal-containing~~ coal formation. Thermal pulse tests performed in situ in a high volatile bituminous C coal at the field pilot site showed a thermal conductivity between 2.0×10^{-3} to 2.39×10^{-3} cal/cm sec °C (0.85 to 1.0 W/(m °K)) at 20 °C. Ranges in these values were due to different measurements between different wells. The thermal diffusivity was 4.8×10^{-3} cm²/s at 20 °C (the range was from about 4.1×10^{-3} to about 5.7×10^{-3} cm²/s at 20 °C). It is believed that these measured values for thermal conductivity and thermal diffusivity are substantially higher than would be expected based on literature sources (e.g., about three times higher in many instances).

On page 244, the two paragraphs beginning on line 10:

Hydrocarbon fluids were produced from a portion of a ~~coal-containing~~coal formation by an in situ experiment conducted in a portion of a ~~coal-containing~~coal formation. The coal was high volatile bituminous C coal. It was heated with electrical heaters. FIG. 136 illustrates a cross-sectional view of the in situ experimental field test system. As shown in FIG. 136, the experimental field test system included at least ~~coal-containing~~coal formation 3802 within the ground and grout wall 3800. ~~Coal-containing~~Coal formation 3802 dipped at an angle of approximately 36° with a thickness of approximately 4.9 meters. FIG. 137 illustrates a location of heat sources 3804a, 3804b, 3804c, production wells 3806a, 3806b, and temperature observation wells ~~3803a~~3808a, 3808b, 3808c, 3808d used for the experimental field test system. The three heat sources were disposed in a triangular configuration. Production well 3806a was located proximate a center of the heat source pattern and equidistant from each of the heat sources. A second production well 3806b was located outside the heat source pattern and spaced equidistant from the two closest heat sources. Grout wall 3800 was formed around the heat source pattern and the production wells. The grout wall may include pillars 1-24. Grout wall 3800 was configured to inhibit an influx of water into the portion during the in situ experiment. In addition, grout wall 3800 was configured to substantially inhibit loss of generated hydrocarbon fluids to an unheated portion of the formation.

Temperatures were measured at various times during the experiment at each of four temperature observation wells 3808a, 3808b, 3808c, 3808d located within and outside of the heat source pattern as illustrated in FIG. 137. The temperatures measured (in degrees Celsius) at each of the temperature observation wells are displayed in FIG. 138 as a function of time. Temperatures at observation wells 3808a (3820), 3808b (3822), and 3808c (3824) were relatively close to each other. A temperature at temperature observation well 3808d (3826) was significantly colder. This temperature observation well was located outside of the heater well triangle illustrated in FIG. 137. This data demonstrates that in zones where there was little superposition of heat, temperatures were significantly lower. FIG. 139 illustrated

illustrates temperature profiles measured at the heat sources 3804a (3830), 3804b (3832), and 3804c (3834). The temperature profiles were relatively uniform at the heat sources.

On page 245, the paragraph beginning on line 23:

Table 5 illustrates the results from analyzing coal before and after it was treated (including heating to the temperatures ~~set forth in~~ as is set forth in FIG. 139 (i.e., after pyrolysis and production of synthesis gas)) as described above. The coal was cored at about 11-11.3 meters from the surface, midway into the coal bed, in both the “before treatment” and “after treatment” examples. Both cores were taken at about the same location. Both cores were taken at about 0.66 meters from well 3804c (between the grout wall and well 3804c) in FIG. 137. In the following Table 5 “FA” means Fisher Assay, “as rec’d” means the sample was tested as it was received and without any further treatment, “Py-Water” means the water produced during pyrolysis, “H/C Atomic Ratio” means the atomic ratio of hydrogen to carbon, “daf” means “dry ash free,” “dmmf” means “dry mineral matter free,” and “mmf” means “mineral matter free.” The specific gravity of the “after treatment” core sample was approximately 0.85 whereas the specific gravity of the “before treatment” core sample was approximately 1.35.

On page 247, the paragraph beginning on line 19:

FIG. 143 illustrates a bar graph of fractions from a boiling point separation of hydrocarbon liquids generated by a Fischer assay and a boiling point separation of hydrocarbon liquids from the coal cube experiment described herein (see, e.g., the system shown in FIG. 129). The experiment was conducted at a much slower heating rate (2 degrees Celsius per day) and the oil produced at a lower final temperature than the Fischer Assay. FIG. 143 shows the weight percent of various boiling point cuts of hydrocarbon liquids produced from a Fruitland high volatile bituminous B coal. Different boiling point cuts may represent different hydrocarbon fluid compositions. The boiling point cuts illustrated include naphtha 3860 (initial boiling point to 166°C), jet fuel 3862 (166°C to 249°C), diesel 3864 (249°C to 370°C), and bottoms 3866 (boiling point greater than 370°C). The hydrocarbon liquids from the coal cube were substantially more valuable products. The API gravity of such hydrocarbon liquids was significantly greater than the API gravity of the Fischer Assay

liquid. The hydrocarbon liquids from the coal cube also included significantly less residual bottoms than were produced from the Fischer Assay hydrocarbon liquids.

On page 248, the paragraph beginning on line 28:

The system depicted in FIG. 89, and the methods of using such system (see other discussion herein with respect to using such system to conduct oil shale experiments) was used to conduct experiments on high volatile bituminous C coal when such coal was heated at 5 °C/day at atmospheric pressure. FIG. 103 depicts certain data points from such experiment (the line depicted in FIG. 103 was produced from a linear regression analysis of such data points). FIG. 103 illustrates the ethene to ethane molar ratio as a function of hydrogen molar concentration in non-condensable hydrocarbons produced from the coal during the experiment. The ethene to ethane ratio in the non-condensable hydrocarbons is reflective of olefin content in all hydrocarbons produced from the coal. As can be seen in FIG. 103, as the concentration of hydrogen autogenously increased during pyrolysis, the ratio of ethene to ethane decreased. It is believed that increases in the concentration (and partial pressure) of hydrogen during pyrolysis causes the olefin concentration to decrease in the fluids produced from pyrolysis.

On page 249, the two paragraphs beginning on line 20:

FIG. 146 illustrates weight percentages of various carbon numbers products removed from high volatile bituminous "C" coal when coal is heated at various heating rates. Data points were derived from laboratory experiments and a Fischer assay. Curves for heating at a rate of 2 °C/day 3870, 3 °C/day 3872, 5 °C/day 3874, and 10 °C/day 3876 provided for similar carbon number distributions in the produced fluids. A coal sample was also heated in a Fischer assay test at a rate of about 17,100 °C/day. The data from the Fischer assay test is indicated by reference numeral 3878. Slow heating rates resulted in less production of components having carbon numbers greater than 20 as compared to the Fischer assay results 3878. Lower heating rates also produced higher weight percentages of components with carbon numbers less than 20. The lower heating rates produced large amounts of components having carbon numbers near 12. A peak in carbon number distribution near 12 is typical of the in situ conversion process for coal and oil shale.

An experiment was conducted on the ~~coal-containing~~coal formation treated according to the in situ conversion process to measure the uniform permeability of the formation after pyrolysis. After heating a portion of the ~~coal-containing~~coal formation, a ten minute pulse of CO₂ was injected into the formation at first production well 3806a and produced at well 3804a, as shown in FIG. 137. The CO₂ tracer test was repeated from production well 3806a to well 3804b and from production well 3806a to well 3804c. As described above, each of the three different heat sources were located equidistant from the production well. The CO₂ was injected at a rate of 4.08 m³/hr (144 standard cubic feet per hour). As illustrated in FIG. 147, the CO₂ reached each of the three different heat sources at approximately the same time. Line 3900 illustrates production of CO₂ at heat source 3804a, line 3902 illustrates production of CO₂ at heat source 3804b, and line 3904 illustrates production of CO₂ at heat source 3804c. As shown in FIG. 149, yield of CO₂ from each of the three different wells was also approximately equal over time. Such approximately equivalent transfer of a tracer pulse of CO₂ through the formation and yield of CO₂ from the formation indicated that the formation was substantially uniformly permeable. The fact that the first CO₂ arrival only occurs approximately 18 minutes after start of the CO₂ pulse indicates that no preferential paths had been created between well 3806a and 3804a, 3804b, and 3804c.

On page 250, the paragraph beginning on line 26:

Synthesis gas was also produced in an in situ experiment from the portion of the ~~coal-containing~~coal formation shown in FIG. 136 and FIG. 137. In this experiment, heater wells were also configured to inject fluids. FIG. 148 is a plot of weight of produced volatiles (oil and noncondensable gas) in kilograms as a function of cumulative energy input in kilowatt hours with regard to the in situ experimental field test. The figure illustrates the quantity and energy content of pyrolysis fluids and synthesis gas produced from the formation.

On page 252, the paragraph beginning on line 4:

FIG. 152 illustrates production rate of synthesis gas (m³/min) as a function of steam injection rate (kg/h) in a coal formation. Data 3930 for a first run corresponds to injection at producer well 3806a in FIG. 137, and production of synthesis gas at heater wells 3804a,

3804b, and 3804c. Data 3932 for a second run corresponds to injection of steam at heater well 3804c, and production of additional gas at a production well 3806a. Data 3930 for the first run corresponds to the data shown in FIG. 151. As shown in FIG. 152, the injected water is in reaction equilibrium with the formation to about 2.7 kg/hr of injected water. The second run results in substantially the same amount of additional synthesis gas produced, shown by data 3932, as the first run to about 1.2 kg/hr of injected steam. At about 1.2 kg/hr, data 3930 starts to deviate from equilibrium conditions because the residence time is insufficient for the additional water to react with the coal. As temperature is increased, a greater amount of additional synthesis gas is produced for a given injected water rate. The reason is that at higher temperatures the reaction rate and conversion of water into synthesis gas increases.

On page 253, the paragraph beginning on line 14:

FIG. 155 is a plot that illustrates the effect of propane injection into a heated coal formation in the experimental field test. Propane was injected into production wells 3806a and 3806b and fluid was produced from heater wells 3804a, 3804b, and 3804c. The average temperatures measured at various wells were as follows: 3804a (737 °C), 3804b (753 °C), 3804c (726 °C), 3808a (589 °C), 3808b (573 °C), 3808c (606 °C), and 3806a (769 °C). When propane contacted the formation, it cracked to produce H₂, methane, ethane, ethene, propylene and coke. FIG. 155 shows that as the propane injection rate increased, the production of H₂ 3960, methane 3962, ethane 3964, ethene 3966, propane 3968, and propylene 3969 increased. This indicates that propane is cracking to form H₂ and lower molecular weight components.

On page 256, the paragraph beginning on line 4:

FIG. 160 is a plot of calculated equilibrium wet mole fractions for a coal reaction with water. Equilibrium wet mole fractions are shown for water 4006, H₂ 4008, carbon monoxide 4010, and carbon dioxide 4012 as a function of temperature at a pressure of 2 bar absolute. At 390 °C, the produced gas includes about 89 % water, about 7 % H₂, and about 4 % carbon dioxide. At 500 °C, the produced gas includes about 66 % water, about 22 % H₂, about 11 % carbon dioxide, and about 1 % carbon monoxide. At 700 °C, the produced gas

includes about percent 18 % water, about 47.5 % H₂, about 12 % carbon dioxide, and about 22.5 % carbon monoxide.

On page 257, the three paragraphs beginning on line 11:

In the embodiments in FIGS. 162-164 the methane reactions in Equations (4) and (5) are included. The calculations set forth herein assume that char is only made of carbon and that there is an excess of carbon to steam. About 890 MWeMW of energy 4024 is required to pyrolyze about 105,800 metric tons per day of coal. The pyrolysis products 4028 include liquids and gases with a production of 23,000 cubic meters per day. The pyrolysis process also produces about 7,160 metric tons per day of water 4030. In the synthesis gas stage about 57,800 metric tons per day of char with injection of 23,000 metric tons per day of steam 4032 and 2,000 MWeMW of energy 4034 with a 20% conversion will produce 12,700 cubic meters equivalent oil per day of synthesis gas 4038.

FIG. 162 is an example of a low temperature in situ synthesis gas production that occurs at a temperature of about 450 °C with heat and mass balances in a hydrocarbon containing formation that was previously pyrolyzed. A total of about 42,900 metric tons per day of water is injected into formation 4100 which may be char. FIG. 162 illustrates that a portion of water 4102 at 25 °C is injected directly into the formation 4100. A portion of water 4102 is converted into steam 4104 at a temperature of about 130 °C and a pressure at about 3 bars absolute using about 1227 MWeMW of energy 4106 and injected into formation 4100. A portion of the remaining steam may be converted into steam 4108 at a temperature of about 450 °C and a pressure at about 3 bars absolute using about 318 MWeMW of energy 4110. The synthesis gas production involves about 23% conversion of 13,137 metric tons per day of char to produce 56.6 millions of cubic meters per day of synthesis gas with an energy content of 5,230 MW. About 238 MW of energy 4112 is supplied to formation 4100 to account for the endothermic heat of reaction of the synthesis gas reaction. The product stream 4114 of the synthesis gas reaction includes 29,470 metric tons per day of water at 46 volume percent, 501 metric tons per day carbon monoxide at 0.7 volume percent, 540 tons per day H₂ at 10.7 volume percent, 26,455 metric tons per day carbon dioxide at 23.8 volume percent, and 7,610 metric tons per day methane at 18.8 volume percent.

FIG. 163 is an example of a high temperature in situ synthesis gas production that occurs at a temperature of about 650 °C with heat and mass balances in a hydrocarbon containing formation that was previously pyrolyzed. A total of about 34,352 metric tons per day of water is injected into formation 4200. FIG. 163 illustrates that a portion of water 4202 at 25 °C is injected directly into formation 4200. A portion of water 4202 is converted into steam 4204 at a temperature of about 130 °C and a pressure at about 3 ~~bar~~bars absolute using about 982 ~~MW~~MW of energy 4206, and injected into formation 4200. A portion of the remaining steam is converted into steam 4208 at a temperature of about 650 °C and a pressure at about 3 ~~bar~~bars absolute using about 413 ~~MW~~MW of energy 4210. The synthesis gas production involves about 22% conversion of 12,771 metric tons per day of char to produce 56.6 millions of cubic meters per day of synthesis gas with an energy content of 5,699 MW. About 898 MW of energy 4212 is supplied to formation 4200 to account for the endothermic heat of reaction of the synthesis gas reaction. The product stream 4214 of the synthesis gas reaction includes 10,413 metric tons per day of water at 22.8 volume percent, 9,988 metric tons per day carbon monoxide at 14.1 volume percent, 1771 metric tons per day H₂ at 35 volume percent, 21,410 metric tons per day carbon dioxide at 19.3 volume percent, and 3535 metric tons per day methane at 8.7 volume percent.

On page 265, the paragraph beginning on line 28:

FIG. 166 is a flowchart of an embodiment of an in situ synthesis gas production process 4510 integrated with a SMDS Fischer-Tropsch and wax cracking process with heat and mass balances. The synthesis gas generating fluid injected into the formation includes about 24,000 metric tons per day of water 4530, which includes about 5,500 metric tons per day of water 4540 recycled from the SMDS Fischer-Tropsch and wax cracking process 4520. A total of about 1700 MW of energy is supplied to the in situ synthesis gas production process 4510. About 1020 MW of energy 4535 of the approximately 1700 MW of energy is supplied by in situ reaction of an oxidizing fluid with the formation, and approximately 680 MW of energy 4550 is supplied by the SMDS Fischer-Tropsch and wax cracking process 4520 in the form of steam. About 12,700 cubic meters equivalent oil per day of synthesis gas 4560 is used as feed gas to the SMDS Fischer-Tropsch and wax cracking process 4520. The

SMDS Fischer-Tropsch and wax cracking process 4520 produces about 4,770 cubic meters per day of products 4570 that may include naphtha, kerosene, diesel, and about 5,880 cubic meters equivalent oil per day of off gas 4580 for a power generation facility.

On page 266, the paragraph beginning on line 22:

The simulation of H₂ 4604 provides a good fit to observed fraction of H₂ 4603. The simulation of methane 4602 provides a good fit to observed fraction of methane 4601. The simulation of carbon dioxide 4606 provides a good fit to observed fraction of carbon dioxide 4605. The simulation of CO 4608 overestimated the fraction of CO 4607 by 4-5 percentage points. Carbon monoxide is the most difficult of the synthesis gas components to model. Also, the carbon monoxide discrepancy may be due to fact that the pattern temperatures exceeded the 550 °C, the upper limit at which the numerical model was calibrated.

On page 269, the paragraph beginning on line 1:

As illustrated in Table 9, pyrolysis of the tar sand decreases nitrogen and sulfur weight percentages in a produced fluid and increases carbon weight percentage in a produced fluid. Increasing the pressure in the pyrolysis experiment appears to further decrease the nitrogen and sulfur weight percentage in the produced fluids.

On page 270, the three paragraphs beginning on line 8:

FIG. 168 illustrates plots of weight percentages of carbon compounds versus carbon number for initial tar 4703 and runs at pressures of 1 bar absolute 4704, 7.9 bars absolute 4705, and 28.6 bars absolute 4706 with a heating rate of 10 °C/day. From the plots of initial tar 4703 and a pressure of 1 bar absolute 4704 it can be seen that pyrolysis shifts an average carbon number distribution to relatively lower carbon numbers. For example, a mean carbon number in the carbon distribution of plot 4703 is at about carbon number nineteen and a mean carbon number in the carbon distribution of plot 4704 is at about carbon number seventeen. Increasing the pressure to 7.9 bars absolute 4705 further shifts the average carbon number distribution to even lower carbon numbers. Increasing the pressure to 7.9 bars absolute 4705 also shifts the mean carbon number in the carbon distribution to a carbon number of about thirteen. Further increasing the pressure to 28.6 bars absolute 4706 reduces

the mean carbon number to about eleven. Increasing the pressure is believed to decrease the average carbon number distribution by increasing a hydrogen partial pressure in the product fluid. The increased hydrogen partial pressure in the product fluid allows hydrogenation, dearomatization, and/or pyrolysis of large molecules to ~~from~~form smaller molecules. Increasing the pressure also increases a quality of the produced fluid. For example, the API gravity of the fluid increased from less than about 10° for the initial tar, to about 31° for a pressure of 1 bar absolute, to about 39° for a pressure of 7.9 bars absolute, to about 45° for a pressure of 28.6 bars absolute.

FIG. 169 illustrates bar graphs of weight percentages of carbon compounds for various pyrolysis heating rates and pressures. Bar graph 4710 illustrates weight percentages for pyrolysis with a heating rate of 1 °C/day at a pressure of 1 bar absolute. Bar graph 4712 illustrates weight percentages for pyrolysis with a heating rate of 5 °C/day at a pressure of 1 bar absolute. Bar graph 4714 illustrates weight percentages for pyrolysis with a heating rate of 10 °C/day at a pressure of 1 bar absolute. Bar graph 4716 illustrates weight percentages for pyrolysis with a heating rate of 10 °C/day at a pressure of 7.9 bars absolute. Weight percentages of paraffins 4720, cycloalkanes 4722, mono-aromatics 4724, di-aromatics 4726, and tri-aromatics 4728 are illustrated in the bar graphs. The bar graphs demonstrate that a variation in the heating rate between 1 °C/day to 10 °C/day does not significantly affect the composition of the product fluid. Increasing the pressure from 1 bar absolute to 7.9 bars absolute, however, affects a composition of the product fluid. Such an effect may be characteristic of the effects described in FIG. 168 and Tables 9 and 10 above.

A three-dimensional (3-D) simulation model was used to simulate an in situ conversion process for a ~~tar sand containing~~tar sand formation. A heat injection rate was calculated using a separate numerical code (CFX). The heat injection rate was calculated at 500 watts per foot (1640 watts per meter). The 3-D simulation was based on a dilation-recompaction model for tar sands. A target zone thickness of 50 meters was used. Input data for the simulation were as follows:

Depth of target zone = 280 meters;



Thickness = 50 meters;
Porosity = 0.27;
Oil saturation = 0.84;
Water saturation = 0.16;
Permeability = 1000 millidarcy;
Vertical permeability versus horizontal permeability = 0.1;
Overburden = shale; and
Base rock = wet carbonate.

Six component fluids were used based on fluids found in Athabasca tar sands. The six component fluids were: heavy fluid; light fluid; gas; water; pre-char; and char. The spacing between wells was set at 9.1 meters on a triangular pattern. Eleven horizontal heaters with a 300 m heater length were used with heat outputs set at the previously calculated value of 1640 watts per meter.